Microwave-cavity measurements for gas thermometry up to the copper point

2013 Metrologia 50 219

(http://iopscience.iop.org/0026-1394/50/3/219)

Metrologia **50** (2013) 219–226 doi:10.1088/0026-1394/50/3/219

Microwave-cavity measurements for gas thermometry up to the copper point

XiaoJuan Feng[1], Keith A Gillis[2], Michael R Moldover[2] and James B Mehl[2,3]

[1] National Institute of Metrology, Beijing 100013, People's Republic of China
[2] National Institute of Standards and Technology, Gaithersburg, MD 20899, USA
[3] 36 Zunuqua Trail, PO Box 307, Orcas, WA 98280, USA

E-mail: fengxj@nim.ac.cn

Received 4 March 2013, in final form 8 April 2013
Published 13 May 2013
Online at stacks.iop.org/Met/50/219

Abstract

This work explores the feasibility of acoustic gas thermometry (AGT) in the range 700 K to the copper point (1358 K) in order to more accurately measure the differences between ITS-90 and the thermodynamic temperature. To test material suitability and stability, we investigated microwave resonances in argon-filled cylindrical cavities machined from a Ni–Cr–Fe alloy. We measured the frequencies of five non-degenerate microwave modes of one cavity at temperatures up to 1349 K using home-made coaxial cables and antennas. The short-term repeatability of both the measured frequencies f_N and the scaled half-widths g_N/f_N was better than 10^{-6} f_N. Oxidation was not a problem while clean argon flowed through the cavity. The measurement techniques are compatible with highly accurate AGT and may be adaptable to refractive index gas thermometry.

(Some figures may appear in colour only in the online journal)

1. Introduction

In 1990, the fractional uncertainty[4] $u(T - T_{90})$ of the International Temperature Scale of 1990 relative to the thermodynamic temperatures T was estimated to increase from 13 mK at the freezing point of zinc (693 K) to 60 mK at the freezing point of copper (1358 K) [1]. In contrast, primary relative acoustic gas thermometry (AGT), as realized at the NIST, achieved smaller uncertainties $u(T - T_{90}) = 2.0$ mK at 551 K [2] and $u(T - T_{90}) = 2.2$ mK at 633 K [3]. In 2011 Fischer *et al* [4] reviewed recent determinations of $(T - T_{90})$ and concluded that the values of $(T - T_{90})$ are near the upper bound of the uncertainty estimated in 1990. However, the recent acoustic measurement at 633 K is well outside the upper uncertainty bound [3]. This unexpected result, together with the high accuracy of primary relative AGT, stimulated the present effort to extend the upper range of AGT from 633 K to the copper point at 1358 K. Fischer *et al* [5] report that the $k = 1$ standard uncertainty for realizing radiation measurements of T_{90} at the reference points is 32 mK in the 'best case'. If AGT can reduce the uncertainty $u(T)$ at the copper point to a value significantly less than 32 mK, $u(T - T_{90})$ could be reduced from 60 mK to a value near 32 mK (by a factor of 0.6) when T_{90} is determined by radiation thermometry at the reference points.

AGT determines the ratio T/T_{ref} of an unknown thermodynamic temperature T to a known, reference temperature T_{ref} from measurements of the acoustic and microwave resonance frequencies of a cavity filled with a noble gas at low density at temperatures T and T_{ref} [6]. In this work, we measured the microwave resonance frequencies of an argon-filled cavity at temperatures near the copper point. The repeatability of both the measured frequencies f_N and the scaled half-widths g_N/f_N was better than 10^{-6} f_N; thus, similar microwave measurements would not limit the precision of AGT at the copper point. The measurement techniques are compatible with the other requirements of AGT, such as maintaining pure gas in the cavity while generating only small, predictable perturbations to both acoustic and microwave frequencies.

For measuring microwave resonance frequencies, we adopted the approach developed by Ripple *et al* [7] for AGT up to 800 K. We used a microwave vector analyser at ambient temperature to generate and detect microwaves

[4] Unless otherwise stated, all uncertainties are one standard uncertainty corresponding to a 68% confidence level.

and home-made coaxial cables to conduct the microwaves to and from an argon-filled cavity at temperatures up to 1349 K. Recently, Ripple *et al* [8] demonstrated that acoustic resonance frequencies could also be measured by generating and detecting sound at ambient temperature and using a duct to conduct sound from the generator to an argon-filled cavity at high temperatures and a second duct to conduct sound out of the cavity to their detector. With suitable duct materials, this scheme will work at any temperature. Cylindrical microwave resonators were used to measure the speed of light [9] and permittivity of gases [10, 11]. Here, we describe the materials and construction techniques that we used to make the coaxial cables and a cylindrical, argon-filled cavity. We tested the system {cables + cavity} at temperatures up to 1349 K.

2. Selection of materials

The metal shell surrounding a high-temperature cavity resonator must be conducting and non-magnetic (to support high-Q microwave resonances without magnetic losses), mechanically stable, resistant to oxidation, capable of being welded, available at a reasonable cost in billets (to make cavity resonators) and in small-diameter tubes and wires (to make acoustic ducts and coaxial cables).

We used the Ni–Fe–Cr alloy HR120 (Haynes International[5], Kokomo, IN, USA) to make the two cylindrical resonators that we tested at high temperatures. For welding, we used another Ni–Fe–Cr alloy available in rod form: Haynes 556. The outer conductors of the coaxial cables were tubes (3.2 mm OD; 2.2 mm ID) of the Ni–Cr–Fe alloy 'Inconel-625' (Special Metals Corp., Huntington, WV, USA). The same tubing stock was used to make the ducts that delivered the argon to the test cavities. The centre conductor of the coaxial cable was a 0.51 mm diameter, 80% Ni:20% Cr (by weight) wire (Alfa Aesar Company, Item Number 13967). Because the thermal expansion of the centre conductor is close to that of the Inconel-625 outer conductor and the HR120 cavity end-plates, the lengths of the antennas protruding into the cavity had only small temperature dependences (figure 1).

When suitable precautions are taken, experience with high-temperature platinum resistance thermometers shows that fused silica with a low OH^- content is a satisfactory insulator at the copper point [3, 12]. To electrically insulate the centre conductor of the coaxial cables from the outer conductor, we used fused silica tubes ('Spectrosil®2000', Quartz Plus Inc. Brookline, NH, USA) alternating with fused silica beads (Swiss Jewel Company, Philadelphia, PA, USA). The silica tubes had an ID of 0.9 mm, an OD of 1.1 mm, and lengths ranging from 6 mm to 25 mm. The silica beads were spherical balls with diameters of 2.00 mm. The manufacturer had drilled a hole through a diameter of each ball. According to the manufacturer, the diameters of the holes were in the range 0.60 mm to 0.68 mm.

[5] In order to describe materials and procedures adequately, it is occasionally necessary to identify commercial products by manufacturers' name or label. In no instance does such identification imply endorsement by China's National Institute of Metrology or the USA's National Institute of Standards and Technology, nor does it imply that the particular product or equipment is necessarily the best available for the purpose.

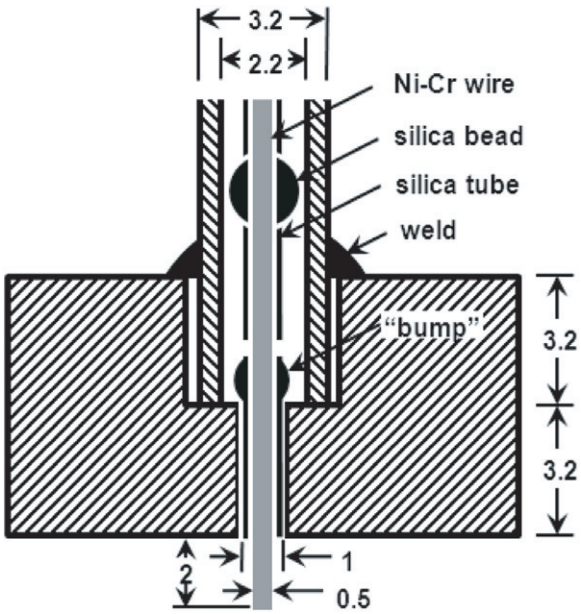

Figure 1. Cross-section (sketch) of coaxial cable terminating in the end of the third test cavity. All dimensions are in millimetres. The centre conductor of one cable extended 2 mm into the cavity to form an antenna; the extension of the second cable was 1 mm. The thicker section of the lowest silica tube acts as a retention ring.

3. Fabrication of coaxial cables and antennas

Figure 1 is a cross-section of the termination of the coaxial cable in the wall of the cavity. The centre conductor of one cable extended 2 mm into the cavity to form a microwave antenna that coupled to the TM modes; the second antenna extended 1 mm into the cavity. Here, we use the notation of [13] and we identify the TM microwave modes by the integers n, m, l, where n is the order of the Bessel function $J_n(x)$ that characterizes the radial dependence of the electric field component E_z, m is the number of zeros (excluding the zero at the origin) in E_z along a radius and l is the number of zeros in the axial component E_z along the length of the cavity. Each antenna was insulated from the hole drilled through the cavity's wall by a specially prepared, fused silica tube. A glass blower had formed a 'bump' near one end to the tube that acted as a retention ring by preventing the tube from falling into the cavity. The annular gaps around the coaxial cables in the walls of an acoustic resonator generate difficult-to-predict perturbations to the acoustic resonance frequencies; therefore, we will avoid them in the future.

Each coaxial cable was assembled in several steps. (1) The outer conductor was welded to the end of the cavity. (2) The centre conductor (nickel–chromium wire) was carefully straightened. The centre conductor wire was threaded through the first silica tube (the one with the bump) and then, alternately, through silica beads and tubes. The lengths of the tubes were deliberately varied in a quasi-random fashion to avoid the coherent reflections that a periodic structure would generate. (3) The wire, now with silica insulators, was threaded through the outer conductor until the first bead reached the shoulder of the hole drilled in the wall of the cavity (figure 1). At this time, the wire and the first

silica tube extended into the cavity. (4) The room-temperature end of the wire and the outer conductor were soldered into a coaxial microwave fitting. (5) The first silica tube was trimmed flush with the inside surface of the cavity's end. (6) The wire was trimmed to its final length to form a straight antenna that coupled to the TM modes. At room temperature, one antenna was 2 mm long and the other was 1 mm long. This length depends on the temperature because of the small difference between the thermal expansion of the nickel–chromium wire and the Inconel outer conductor and the HR120 end-plate. With the present antennas, the microwave signal-to-noise ratios ranged from 1300 to 3400. In the future, we will use flush antennas, such as those described in [14]. The weaker coupling between the flush antennas and the cavity will reduce the signal-to-noise ratios; however, the resonance frequencies will be less sensitive to small motions of the flush antennas relative to the flanges supporting them.

A perfectly conducting, vacuum-insulated, coaxial cable with the present dimensions ($r_a = 0.25$ mm, $r_b = 1.1$ mm) has a capacitance per unit length of $C = 37.5\,\mathrm{pF\,m^{-1}}$, an inductance per unit length $\mathcal{L} = 0.296\,\mu\mathrm{H\,m^{-1}}$, a characteristic impedance $Z_c = (\mathcal{L}/C)^{1/2} = 88.8\,\Omega$ and a propagation speed $v = c = (\mathcal{L}C)^{-1/2}$. The beads and spacers do not change $\mathcal{L}$; however, they increase the average value of C to $C' \approx 44.0\,\mathrm{pF\,m^{-1}}$, as estimated using finite element calculations. All the modes of a cable with an inhomogeneous dielectric are hybrid modes; full characterization of the hybrid modes for our design is beyond the scope of this paper. However, the silica beads and spacers only occupy 14% of the cable's volume; therefore, a reasonable approximation is to assume that the dominant mode is nearly a TEM mode with a characteristic impedance $Z_c = (\mathcal{L}/C')^{1/2} = 82.1\,\Omega$ and a propagation speed $v = c(C/C')^{1/2} = 0.924\,c$. Figure 2 compares the transmission coefficients $S21$ of 30 cm lengths of home-made coaxial cable and commercially manufactured cable, as measured by a microwave vector analyser. For the home-made cable, the values of $S21$ indicate reflections at multiples of 460 MHz. These reflections are consistent with one half of a wavelength fitting within 30 cm of the cable and a propagation speed $0.924\,c$. These reflections reduce the signal-to-noise ratio; however, they did not cause other problems when fitting the cavity's resonances because the 460 MHz periodicity of the reflections is much larger than the half-widths (0.8 MHz to 2.2 MHz) of the microwave modes that we used. Using the commercially manufactured cables and again using the home-made cables, we measured the half-widths of five TM(0, 1, l) modes ($l = 0$, 1, 2, 3, 4) of the first test cavity described below at ambient temperature. We found $10^6(g_{\text{home-made}} - g_{\text{commercial}})/f = 0.12 \pm 0.50$ and $10^6(f_{\text{home-made}} - f_{\text{commercial}})/f = -1.60 \pm 0.38$. (The indicated uncertainty is one standard deviation.) Thus, the home-made cables made an insignificant contribution to the measured half-widths. These comparison measurements were made without a thermostat; therefore, the small frequency change probably resulted from a small temperature change.

We estimated the coupling of the antennas to the cavity using the formalism of Underwood *et al* [14]. The charge q_{tip} accumulated on the ends of the antennas was calculated using finite elements; it can be expressed using equation (24) of [14] by replacing the constant 0.756 with 22.4 for our shorter probe antenna and with 104 for our longer probe antenna. In their notation, our value of r_h is 0.5 mm. We cannot accurately calculate the external contribution to $1/Q$ from the value of q_{tip} without a better understanding of the cable modes. If we make the crude assumption that the cable presents only a resistive load of 50 Ω, we find $1/Q_{\text{ext}} \approx 0.2/Q$.

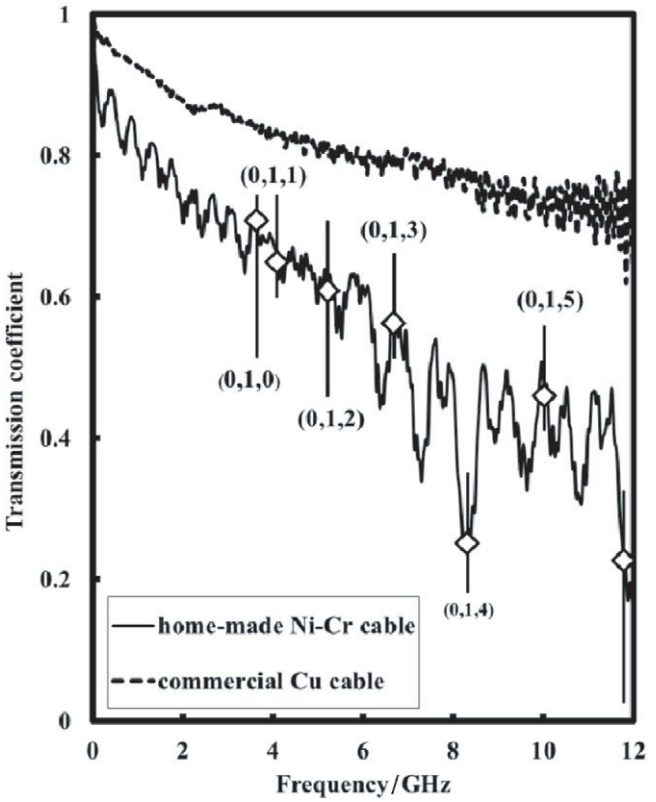

Figure 2. Transmission coefficients of cables. The vertical lines are not measurements; they indicate the frequencies of the modes reported here.

4. Three test resonators

We built three cylindrical cavities. The first one was used for room-temperature tests of the home-made microwave cables and for room-temperature tests of suitability of the alloy HR120 for the walls of a cavity resonator. The second resonator was used to test for oxidation at high temperatures. We used the third resonator to demonstrate the feasibility of measuring microwave resonance frequencies and half-widths at temperatures up to 1349 K, the highest temperature reached by our small, horizontal tube furnace.

The first test resonator had an ID of 63 mm and a length of 80 mm. Its end-plates were sealed to its tubular body with bolts that compressed indium O-rings. We identified the frequencies of the lowest 30 microwave modes of the cavity. When confronting these data, we were reminded that the TE(0, 1, l) modes of a cylinder are degenerate with TM(1, 1, l) modes. Here and below, we report results only for the five non-degenerate modes TM(0, 1, l) for $l = 0$, 1, 2, 3 and 4. Table 1 summarizes some of the test results. For table 1, the calculated

Table 1. Results from first (indium-sealed) test resonator at 22 °C. ($\Delta f \equiv f_{\rm meas} - f_{\rm calc}$; $\Delta g \equiv g_{\rm meas} - g_{\rm calc}$.)

TM mode	$f_{\rm meas}$/MHz	$g_{\rm meas}$/MHz	Q	$10^6\Delta f/f_{\rm meas}$	$10^6\Delta g/f_{\rm meas}$	$g_{\rm meas}/g_{\rm calc}$
(0, 1, 0)	3641.82	0.739	2463	−58	14	1.074
(0, 1, 1)	4093.31	1.003	2040	79	17	1.073
(0, 1, 2)	5217.45	1.132	2304	−1	15	1.072
(0, 1, 3)	6683.60	1.283	2605	−9	13	1.074
(0, 1, 4)	8312.69	1.429	2909	−5	12	1.072

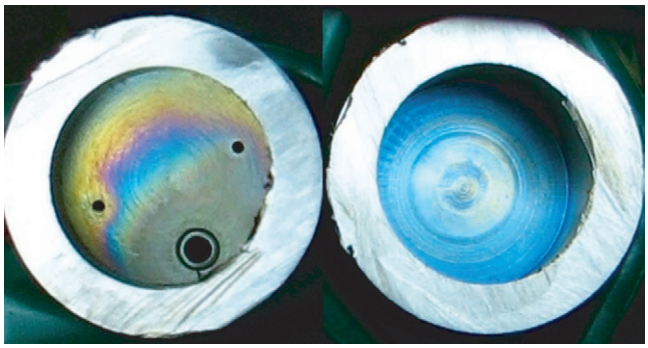

Figure 3. Small test cavity after exposure to 45 mol of argon for 15 h at temperatures ranging from 870 K to 1270 K. The argon entered through the 2.2 mm ID tube at the left and exited through the two 1.0 mm diameter ports that led to the coaxial cables.

frequencies $f_{\rm calc}$ were obtained by varying the length ($L = 80.2391$ mm) and radius of the cavity ($a = 31.5061$ mm) to minimize the sum $\Sigma[(f_{\rm meas} + g_{\rm calc})/(f_{\rm calc} + g_{\rm calc}) - 1]^2$. We used the resistivity of the alloy HR120 (105 μΩ cm at 20 °C) provided by the manufacturer to calculate the half-widths $g_{\rm calc}$. As shown in the last column of table 1, all the values of $g_{\rm meas}/g_{\rm calc}$ were remarkably close to 1.073. This suggests that the resistivity of our sample is 14% higher than that stated by the manufacturer. We conclude that the alloy HR120 did not generate large, unexpected microwave losses at the boundary (e.g. from magnetic hysteresis) that would be incompatible with accurate AGT.

For high-temperature AGT, we note that the resistivity of HR120 increases only 22% when the temperature is raised from 293 K to 1473 K. Theoretically, the microwave Qs of the TM modes of a cylindrical cavity with an ID equal to its length are approximately the same as the Qs of the modes in a quasi-spherical cavity of equal volume. Therefore, the Qs that we measured (2040 to 2909) can be achieved using a quasi-spherical cavity designed for AGT.

The second cavity resonator was used to test for oxidation at high temperatures. It had an ID of 16.8 mm and a length of 33 mm. We heated this small cavity resonator in a tube furnace to 1270 K in two runs with interleaving steps of 200 K, spending approximately 3 h at each step. During this process, approximately 3 mol h^{-1} of argon (research grade; 99.9995% argon by volume) flowed into the cavity through a port (2.2 mm ID) and out through coaxial cables. Thus, the cavity was exposed to 45 mol of argon while at 870 K or higher. After these thermal cycles, the outside of the cavity, the coaxial cables and the welds were covered with a dark grey oxide. We sawed the cavity into two parts and photographed its inner surfaces using white light. As shown in figure 3 (right), the metal surface facing the inflowing argon had turned blue. As shown in figure 3 (left), the metal surface between the gas inlet and one outlet had no distinct colour. However, the surface surrounding the second outlet tube had become yellow. These white light fringes suggest that Cr_2O_3 films [15] of the order of 250 nm thick had formed while the cavity was hot. If we had passed the argon through a getter, the oxide films probably would have been thinner. If thick oxide films are formed during AGT and if they are ignored, they may lead to errors of order (film thickness)/(cavity dimension) because the acoustic dimensions will differ from the microwave dimensions. However, thick oxide films can be detected by comparing TE modes and TM modes in a quasi-spherical cavity [16].

For most of our frequency measurements, we used the third cylindrical resonator shown in figure 4. Its cavity had a length of 80 mm, a diameter of 63 mm, and its walls were 6.4 mm thick. The interior surfaces were not polished. The end-plates of the third resonator had annular gaps where the gas inlet and outlet ducts terminated at the boundary of the cavity (see figure 3, left, for a similar annular gap).

In contrast with the first resonator that was bolted together, the ends of the third resonator were welded to its body and the half-widths of the microwave modes were 19% to 72% larger than those predicted (table 2) from the resistivity of the alloy HR120. This unexpected result was a concern because determining the thermal expansion of the cavity from the measured microwave frequencies requires a correction for the microwave penetration depth $\delta_{\rm m}$ which is usually determined from the measured half-widths. (In this work, $6\,\mu{\rm m} < \delta_{\rm m} < 9\,\mu{\rm m}$ and the length corrections are of the order of $1.4 \times 10^{-4} < 2\delta_{\rm m}/L < 3.0 \times 10^{-4}$.)

The resonance widths measured with the third resonator exceed those measured with the first resonator by 12% for the TM010 mode, rising monotonically to 61% for the TM014 modes. Finite-element simulations of cavities with a concentric slot at the junction between the sides and top show similar behaviour. It is highly plausible that the excess widths of the third resonator are due to the open gap.

In an effort to understand the excess half-widths of the welded resonator, we sawed it apart after completing the microwave measurements at high temperatures. The interior surfaces had no signs of oxidation, except for a hazy circle, approximately 15 mm in diameter, surrounding the 2.2 mm ID gas inlet duct. We found that the weld that joined each end-plate to the body of the cavity had penetrated approximately 1.5 mm. Wedge-shaped gaps had formed during the welding between each end-plate and the body of the resonator. The apex of the gap was close to the weld and the gap widened towards the inside of the cylinder. The combined area of both gaps (counting both surfaces of each gap) might have been as large as 25% of the area of the cylindrical cavity. Because

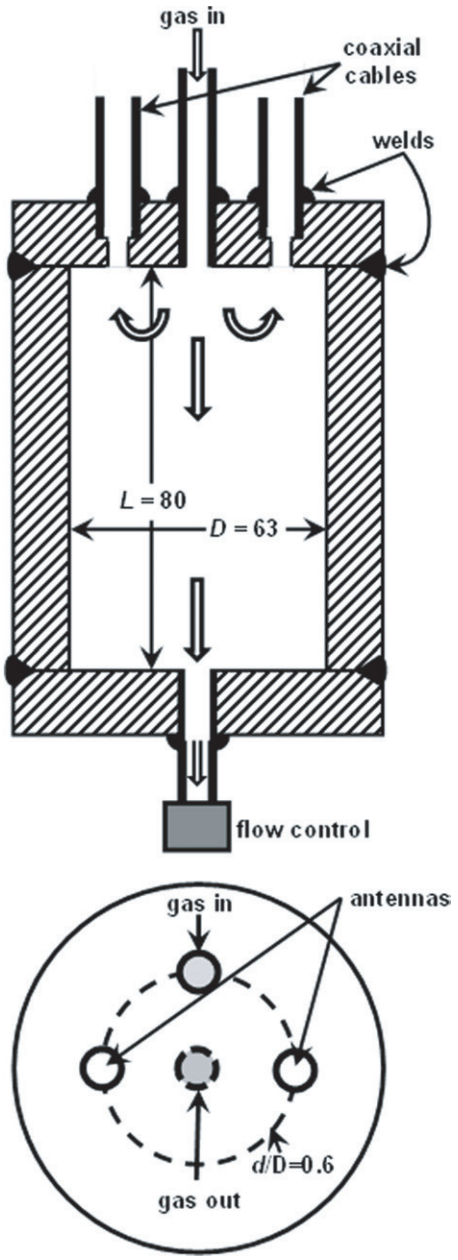

Figure 4. Sketch of the resonator showing the location of coaxial cables and ducts that supply and remove argon. All dimensions are in millimetres.

these gaps occurred in a region of high current for TM(0, 1, l) modes, they may have significantly decreased the Qs of these modes. The width of each gap varied around the circumference of the cavity and reached a maximum of approximately 8 µm. We estimate that the combined volume of the gaps was only 4×10^{-6} of the volume of the cavity. If the volume of the gaps were stable, its contribution to the uncertainty of relative AGT would be negligible because such gaps have only small effects on the microwave and acoustic resonance frequencies.

5. High-temperature measurements

All the high-temperature microwave measurements with the third resonator (figure 4) were made in a simple, horizontal tube furnace. During the measurements, an argon pressure of 133 kPa was maintained in the cavity and argon flowed through the cavity at approximately 0.3 mol h^{-1}. (Most of the argon flowed from the inlet to the outlet; however, a small fraction of it leaked out through the coaxial cables.) The microwave data were acquired during four runs, each lasting more than 12 h, as shown at the bottom of figure 5. These measurements provided information about signal-to-noise ratios, short-term dimensional stability of the cavity and the dimensional changes resulting from temperature cycling. We discuss these results in order.

At ambient temperature, the microwave resonance frequencies f_{mnl} and scaled half-widths g_{mnl}/f_{mnl} were measured with an uncertainty of 10^{-7} f_{mnl} or less in 20 s using a commercial vector analyser. At higher temperatures, the uncertainty of the frequency measurements was dominated by fluctuations in the temperature of the furnace, as illustrated in figure 6 with 40 min of data at 976 K and 1349 K. In figure 6, the frequency tracks the temperature with a delay of approximately 1 min. However, the amplitude of the frequency fluctuations is smaller than the product (temperature fluctuations)×(coefficient of thermal expansion). This occurred because the temperature was measured using a thermocouple that was located just outside the resonator, where it responded quickly to the temperature fluctuations, whereas the resonance frequency depended on the average temperature of the resonator, which had a slower response. The data shown from 18 January 2012 at 976 K have a fractional standard deviation (FSD) from the mean of 6.6×10^{-7}. This decreased to 5.2×10^{-7} when a linear function of the temperature was subtracted from the frequency measurements. The frequency data at 1349 K from 23 January 2012 had the FSD from the mean of 1.5×10^{-6} after we removed a linear function of the temperature and a fractional time dependence of 34×10^{-6} h^{-1} from the data. (Selected 10 min long segments at 1349 K had FSDs of 1.0×10^{-6}.) From these data, we conclude that the signal-to-noise ratio and short-term frequency stability are suitable for highly accurate AGT.

As the temperature was increased from 295 K to 1349 K, the Qs decreased by 5% to 16%; however, the signal-to-noise ratio *increased* by 25% to 70%. This unexpected result might indicate that the coupling of the antennas to the cavity increased as the temperature increased. While the temperature of the resonator increased, we observed occasional, sudden (within 1 s), small (e.g. 2%) increases in the amplitude of the detected microwave signal. We speculate that these amplitude changes were caused by abrupt motions of the centre conductor of a coaxial cable moving further into the cavity.

As shown in figure 5, the maximum temperatures in the measurement cycles were 1177 K, 1274 K, 1178 K and 1349 K. The top and centre panels of figure 5 display the effects of temperature cycling on the frequencies and half-widths of the modes studied. We expected the cavity's dimensions to change during the first run up to 1177 K because the welding left substantial stress in the resonator. Unfortunately, the frequencies and half-widths changed during every run. For example, the half-widths decreased approximately 1% during the third run even though the maximum temperature was 96 K

Table 2. Data from the third test resonator during the third heating cycle.

TM mode	f_{meas}/MHz	g_{meas}/MHz	Q	$10^6\Delta f/f_{meas}$	$10^6\Delta g/f_{meas}$	g_{meas}/g_{calc}
			at 370.6 K			
(0, 1, 0)	3635.767	0.852	2134	70	40	1.21
(0, 1, 1)	4088.000	1.263	1619	−68	75	1.32
(0, 1, 2)	5215.980	1.462	1784	−63	73	1.36
(0, 1, 3)	6686.256	1.745	1916	26	79	1.43
(0, 1, 4)	8318.761	2.221	1873	35	112	1.73
			at 1177.9 K			
(0, 1, 0)	3581.501	0.905	1979	64	40	1.19
(0, 1, 1)	4027.038	1.346	1496	−61	78	1.30
(0, 1, 2)	5138.208	1.558	1649	−62	77	1.34
(0, 1, 3)	6586.586	1.859	1772	26	83	1.41
(0, 1, 4)	8194.772	2.388	1716	32	122	1.72

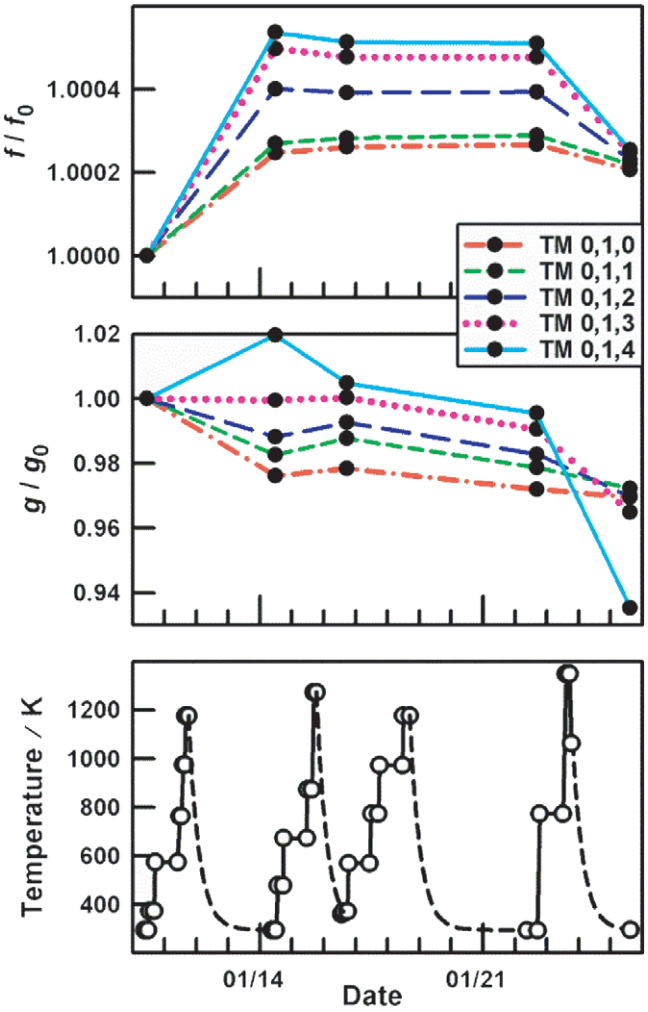

Figure 5. Bottom: temperature–time history of the third test resonator. The circles bound constant-temperature intervals when frequencies were measured. Frequencies were not measured while cooling (dashed curves). Middle: half-widths at 294 K divided by the half-widths first measured at 294 K. Top: resonance frequencies at 294 K divided by the frequencies first measured at 294 K. When the resonator was exposed to high temperatures, the cavity's dimensions appeared to change by as much as 0.04%.

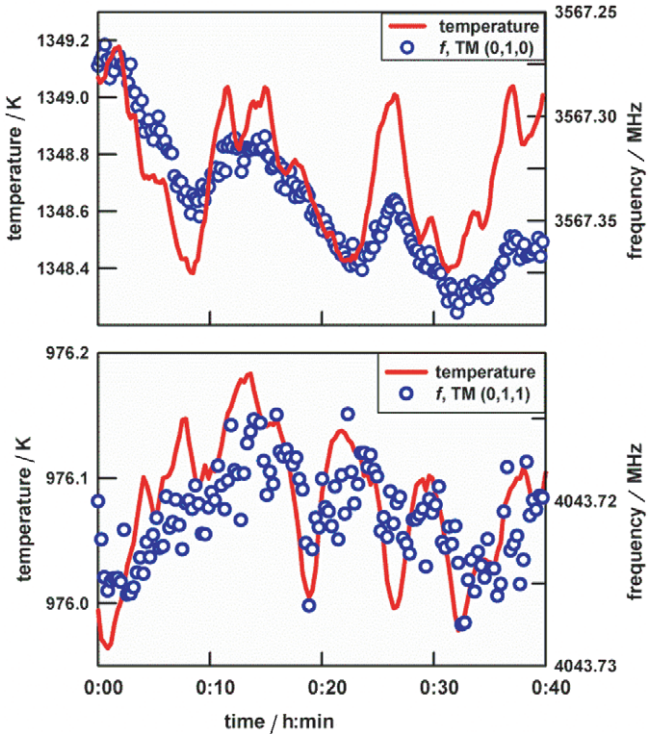

Figure 6. Solid curves: temperature as a function of elapsed time. Points: measured frequency as a function of elapsed time. Note that the frequency scales on the right decrease towards the top of the graph.

less than the maximum temperature during the second run (figure 5, middle panel).

Table 2 lists some of the data acquired during the third run using the third resonator. We fitted the cavity's length and radius to the values of (f_{meas} + g_{calc}) as described above. The residuals from the fitting $\Delta f/f_{meas}$ and $\Delta g/f_{meas}$ in table 2 are much larger than the corresponding residuals for the O-ring sealed resonator (table 1). Also, the temperature dependence of the residuals is very small. In other words, the modes of the welded resonator are more strongly perturbed from the modes of an ideal cylinder than the modes of the O-ring sealed resonator; however, perturbations are nearly independent of temperature.

The last column of table 2 shows that the ratios g_{meas}/g_{calc} are nearly independent of the temperature or, equivalently, the temperature dependence is consistent with the resistivity of the alloy. This suggests that the excess half-widths result from geometric features such as surface roughness or crevices where the cavity's ends and sides are joined.

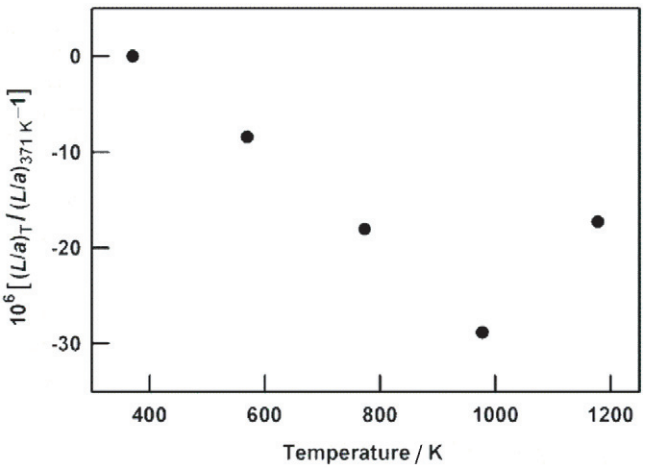

Figure 7. Temperature dependence of ratio (length)/(radius) for the third test cavity during the third temperature cycle. The vertical scale is in parts per million.

The present exploratory measurements are not suitable for accurately determining the thermal expansion of the acoustic cavity between an unknown temperature T and a known reference temperature $T_{\rm ref}$. However, the present measurement determines the temperature dependence of the ratio L/a, a quantity that would be independent of the temperature if the thermal expansion of the cavity were isotropic. Figure 7 displays the temperature dependence of this ratio during the third run. The determinations of $(L/a)_T/(L/a)_{370.6\,\rm K}$ up to 977.7 K fall within 0.5×10^{-6} of a straight line; however, the measurement at 1177.9 K departs from the line by 20.6×10^{-6}. This suggests that the thermal expansion of the third resonator during the third run was a smooth function of the temperature over a wide enough range to be useful for AGT.

6. Discussion

We reported progress towards a new generation of acoustic/microwave cavity resonators operating at temperatures up to the copper point 1358 K. Suitable, non-magnetic materials are available. Oxidation was not a problem when clean argon flowed through the cavity. Microwave signal-to-noise ratios were satisfactory (>1000). The conductors comprising the horizontal microwave cables did not sag enough to short and we did not detect problems attributable to insulation leakage. To summarize, we have successfully demonstrated the viability that microwave measurements will not contribute significant uncertainties to high-temperature AGT if the temperature dependence of the half-widths can be understood with an uncertainty of the order of 0.1% of the half-widths.

At ambient temperature, the values of Δf and Δg obtained with the welded resonator were much larger than the values of Δf and Δg obtained with the bolted-together resonator, even though both resonators were made of the same alloy and machined to the same tolerances. If welded construction is desired, this problem could be greatly reduced by locating the weld(s) where the currents of selected microwave modes vanish. For example, consider a cylindrical resonator assembled from two identical parts, where each part is an end-plate with a cylindrical extension. When the identical cylindrical extensions are joined, perhaps by a weld, the resulting cavity has a seam that is perpendicular to the cavity's axis and located where the currents associated with the TM(0, 1, l) modes vanish. Furthermore, any gap at that location could be reduced by exploiting the deeper penetration available from electron-beam welding. Alternatively, the cavity could be assembled by bolting the two parts together and placing the assembled resonator within a separate pressure vessel. In fact, this approach has been used for AGT conducted with quasi-spherical cavity resonators at lower temperatures [6].

We can consider using the present coaxial cables, microwave cavity and argon flow system to realize primary refractive index gas thermometry (RIGT) at microwave frequencies and temperatures up to the copper point. Upon comparing AGT and RIGT at a given temperature, one finds that RIGT generally requires purer gas, a cavity with greater dimensional stability and operation at higher densities (and therefore higher pressures). Similar considerations apply to realizing dielectric constant gas thermometry at high temperatures, where the requirement for greater dimensional stability applies to the capacitor(s) instead of to the microwave cavity.

Acknowledgments

The authors thank Jim Schmidt, Wes Tew, Dean Ripple, Greg Strouse for their advice, Karen Garrity for thermocouple calibrations, Jeffrey Anderson for modifying silica insulators, John Jendzursk for the use of a microwave vector analyser, and Keith Moore from Haynes International Inc. for providing alloy samples. XiaoJuan Feng was supported by the National Natural Science Foundation of China (Grant No 51106143, No 51276175 and No 61001034).

References

[1] BIPM 1990 *Supplementary Information for the International Temperature Scale of 1990* (Sèvres, France: Bureau International des Poids et Mesures) p 13
[2] Ripple D C, Strouse G F and Moldover M R 2007 *Int. J. Thermophys.* **28** 1789–99
[3] Strouse G F 2013 private communication
[4] Fischer J, de Podesta M, Hill K D, Moldover M R, Pitre L, Rusby R, Steur P, Tamura O, White R and Wolber L 2011 *Int. J. Thermophys.* **32** 12–25
[5] Fischer J *et al* 2003 *Uncertainty Budgets for Realisation of Scales by Radiation Thermometry* Document CCT/03-03 available at www.bipm.org/cc/CCT/Allowed/22/CCT03-03.pdf
[6] Moldover M R, Gavioso R M, Mehl J B, Pitre L, de Podesta M and Zhang J 2012 Mise en Practique *Thermodynamic temperature measurement by acoustic gas thermometry: Appendix* Bureau International des Poids et Measures, www.bipm.org/utils/en/pdf/MeP_K.pdf
[7] Ripple D C, Defibaugh D R, Moldover M R and Strouse G F 2003 *8th Int. Temperature Symp. (Chicago, IL, 21–24 October 2002) Temperature: Its Measurement and Control in Science and Industry* vol VII, ed D C Ripple (Melville, NY: American Institute of Physics) pp 25–30
[8] Ripple D C, Strouse G F, Gillis K A and Moldover M R 2012 *Proc. 9th Int. Temperature Symp. (19–23 March 2012,*

Anaheim, CA) (Melville, NY: American Institute of Physics) at press
[9] Essen L and Gordon-Smith A C 1948 *Proc. R. Soc.* A **194** 348
[10] Ewing M B and Royal D D 2002 *J. Chem. Thermodyn.* **34** 1073–88
[11] Ewing M B and Royal D D 2002 *J. Chem. Thermodyn.* **34** 1985–99
[12] Strouse G F, Mangum B W, Pokhodun A I and Moiseeva N P 1992 *Proc. 7th Int. Temperature Symp. (Toronto, Ontario, Canada, 28 April–1 May 1992) Temperature: Its Measurement and Control in Science and Industry* vol 6, ed J F Schooley (Melville, NY: American Institute of Physics) pp 389–94
[13] Collin R E 1992 *Foundations of Microwave Engineering* 2nd edn (New York: McGraw-Hill)
[14] Underwood R J, Mehl J B, Pitre L, Edwards G, Sutton G and de Podesta M 2010 *Meas. Sci. Technol.* **21** 075103
[15] Gleesom B and Harper M A 1998 *Oxid. Met.* **49** 373–99
[16] May E F, Pitre L, Mehl J B, Moldover M R and Schmidt J W 2004 *Rev. Sci. Instrum.* **75** 3307–17